their behaviors as radioligands for PK binding sites in rats. Nucl Med Biol. 1994;21:573–81.
12. Belloli S, Moresco RM, Matarrese M, Biella G, Sanvito F, Simonelli P, et al. Evaluation of three quinoline carboxamide derivatives as potential radioligands for the in vivo PET imaging of neurodegeneration. Neurochem Int. 2004;44:433–40.
13. Petit-Taboué MC, Baron JC, Barré L, Travère JM, Speckel D, Camsonne R, et al. Brain kinetics and specific binding of [^{11}C]PK 11195 to omega 3 sites in baboons: positron emission tomography study. Eur J Pharmacol. 1991;200:347–51.
14. Kropholler MA, Boellaard R, Schuitemaker A, van Berckel BN, Luurtsema G, Windhorst AD, et al. Development of a tracer kinetic plasma input model for (*R*)-[11C]PK11195 brain studies. J Cereb Blood Flow Metab. 2005;25:842–51.
15. Lockhart A, Davis B, Matthews JC, Rahmoune H, Hong G, Gee A, et al. The peripheral benzodiazepine receptor ligand PK11195 binds with high affinity to the acute phase reactant alpha1-acid glycoprotein: implications for the use of the ligand as a CNS inflammatory marker. Nucl Med Biol. 2003;30:199–206.
16. Zhang M-R, Kida T, Noguchi J, Furutsuka K, Maeda J, Suhara T, et al. [^{11}C]DAA1106: radiosynthesis and in vivo binding to peripheral benzodiazepine receptors in mouse brain. Nucl Med Biol. 2003;30:513–9.
17. Zhang MR, Maeda J, Ogawa M, Noguchi J, Ito T, Yoshida Y, et al. Development of a new radioligand, *N*-(5-fluoro-2-phenoxyphenyl)-*N*-(2-[^{18}F]fluoroethoxyl-5-methoxy benzyl)acetamide, for PET imaging of peripheral benzodiazepine receptor in primate brain. J Med Chem. 2004;47:2228–35.
18. Briard E, Zoghbi S, Imaizumi M, Gourley J, Shetty U, Hong J, et al. Synthesis and evaluation of two sensitive ^{11}C-labeled aryloxyanilide ligands for imaging brain peripheral benzodiazepine receptors in vivo. J Med Chem. 2008;51:17–30.
19. Wilson A, Garcia A, Parkes H, McCormick P, Stephenson K, Houle S, et al. Radiosynthesis and initial evaluation of [^{18}F]-FEPPA for PET imaging of peripheral benzodiazipine receptors. Nucl Med Biol. 2008;35:305–14.
20. James M, Fulton R, Henderson D, Eberl S, Meikle S, Thomson S, et al. Synthesis and in vivo evaluation of a novel peripheral benzodiazepine receptor PET radioligand. Bioorg Med Chem. 2005;13:6188–94.
21. Martín A, Boisgard R, Thézé B, Van Camp N, Kuhnast B, Damont A, et al. Evaluation of the PBR/TSPO radioligand [(18)F]DPA-714 in a rat model of focal cerebral ischemia. J Cereb Blood Flow Metab. 2010;30:230–41.
22. Zhang M, Kumata K, Maeda J, Yanamoto K, Hatori A, Okada M, et al. ^{11}C-AC-5216: a novel PET ligand for peripheral benzodiazepine receptors in the primate brain. J Nucl Med. 2007;48:1853–61.
23. Mattner F, Mardon K, Katsfis A. Pharmacological evaluation of [^{123}I]-CLINDE: a radioiodinated imidazopyridine-3-acetamide for the study of peripheral benzodiazepine binding sites (PBBS). Eur J Nucl Med Mol Imaging. 2008;35:779–89.
24. Sekimata K, Hatano K, Ogawa M, Abe J, Magata Y, Biggio G, et al. Radiosynthesis and in vivo evaluation of *N*-[^{11}C]methylated imidazopyridineacetamides as PET tracers for peripheral benzodiazepine receptors. Nucl Med Biol. 2008;35:327–34.
25. Denora N, Laquintana V, Pisu MG, Dore R, Murru L, Latrofa A, Trapani G, Sanna E. 2-Phenyl-imidazo[1,2-a]pyridine compounds containing hydrophilic groups as potent and selective ligands for peripheral benzodiazepine receptors: synthesis, binding affinity and electrophysiological studies. J Med Chem. 2008;2008(51):6876–87.
26. Toyama H, Hatano K, Suzuki H, Ichise M, Momosaki S, Kudo G, et al. In vivo imaging of microglial activation using a peripheral benzodiazepine receptor ligand: [^{11}C]PK-11195 and animal PET following ethanol injury in rat striatum. Ann Nucl Med. 2008;22:417–24.
27. Bergeron M, Cadorette J, Beaudoin JF, Lepage MD, Robert G, Selivanov V, et al. Performance evaluation of the LabPET APD-based digital PET scanner. IEEE Trans Nulc Sci. 2009;56:10–6.
28. Converse AK, Larsen EC, Engle JW, Barnhart TE, Nickles RJ, Duncan ID. ^{11}C-(R)-PK11195 PET imaging of microglial activation and response to minocycline in Zymosan-treated rats. J Nucl Med. 2011;52:257–62.
29. Logan J, Fowler JS, Volkow ND, Wang GJ, Ding YS, Alexoff DL. Distribution volume ratios without blood sampling from graphical analysis of PET data. J Cereb Blood Flow Metab. 1996;16:834–40.
30. Lawson LJ, Perry VH, Dri P, Gordon S. Heterogeneity in the distribution and morphology of microglia in the normal adult mouse brain. Neurosci. 1990;39:151–70.
31. Chen MK, Baidoo K, Verina T, Guilarte TR. Peripheral benzodiazepine receptor imaging in CNS demyelination: functional implications of anatomical and cellular localization. Brain. 2004;127:1379–92.
32. Boutin H, Chauveau F, Thominiaux C, Gregoire MC, James ML, Trebossen R, Hantraye P, Dolle F, Tavitian B, Kassiou M. ^{11}C-DPA-713: a novel peripheral benzodiazepine receptor PET ligand for in vivo imaging of neuroinflammation. J Nucl Med. 2007;48:573–81.
33. Yasuno F, Kosaka J, Ota M, Higuchi M, Ito H, Fujimura Y, Nozaki S, Takahashi S, Mizukami K, Asada T, Suhara T. Increased binding of peripheral benzodiazepine receptor in mild cognitive impairment-dementia converters measured by positron emission tomography with [(11)C]DAA1106. Psychiatry Res. 2012;203:67–74.
34. Fujita M, Imaizumi M, Zoghbi SS, Fujimura Y, Farris AG, Suhara T, Hong J, Pike VW, Innis RB. Kinetic analysis in healthy humans of a novel positron emission tomography radioligand to image the peripheral benzodiazepine receptor, a potential biomarker for inflammation. Neuroimage. 2008;40:43–52.
35. Owen DR, Howell OW, Tang SP, Wells LA, Bennacef I, Bergstrom M, Gunn RN, Rabiner EA, Wilkins MR, Reynolds R, Matthews PM, Parker CA. Two binding sites for [^{3}H]PBR28 in human brain: implications for TSPO PET imaging of neuroinflammation. J Cereb Blood Flow Metab. 2010;30(9):1608–18.

Journal of Alzheimer's Disease xx (20xx) x–xx
DOI 10.3233/JAD-141338
IOS Press

Prediction of Outcomes in Mild Cognitive Impairment by Using ^{18}F-FDG-PET: A Multicenter Study

Kengo Ito[a,b,*], Hidenao Fukuyama[c], Michio Senda[d], Kazunari Ishii[e], Kiyoshi Maeda[f], Yasuji Yamamoto[g], Yasuomi Ouchi[h], Kenji Ishii[i], Ayumu Okumura[j], Ken Fujiwara[a], Takashi Kato[a], Yutaka Arahata[k], Yukihiko Washimi[k], Yoshio Mitsuyama[l], Kenichi Meguro[m], Mitsuru Ikeda[n] and SEAD-J Study Group

[a]*Department of Clinical and Experimental Neuroimaging, National Center for Geriatrics and Gerontology, Obu-shi, Aichi, Japan*
[b]*Department of Radiology, National Center for Geriatrics and Gerontology, Obu-shi, Aichi, Japan*
[c]*Human Brain Research Center, Kyoto University, Kyoto, Japan*
[d]*Division of Molecular Imaging, Institute of Biomedical Research and Innovation, Kobe, Japan*
[e]*Department of Radiology, Kinki University, Osaka, University*
[f]*Department of Medical Rehabilitation, Kobe Gakuin University, Kobe, Japan*
[g]*Department of Psychiatry, Kobe University Graduate School of Medicine, Kobe, Japan*
[h]*Medical Photonics Research Center, Hamamatsu University School of Medicine, Hamamatsu, Japan*
[i]*Positron Medical Center, Tokyo Metropolitan Institute of Gerontology, Tokyo, Japan*
[j]*Chubu Medical Center for Prolonged Traumatic Brain Dysfunction, Kizawa Memorial Hospital, Gifu, Japan*
[k]*National Hospital for Geriatric Medicine, National Center for Geriatrics and Gerontology, Obu-shi, Aichi, Japan*
[l]*Psychogeriatric Center, Daigo Hospital, Miyazaki, Japan*
[m]*Department of Geriatric Behavioral Neurology, Tohoku University Graduate School of Medicine, Miyagi, Japan*
[n]*Department of Radiological Technology, Nagoya University School of Health Sciences, Nagoya, Japan*

Handling Associate Editor: Henryk Barthel

Accepted 12 December 2014

Abstract.
Background: ^{18}F-FDG-PET is defined as a biomarker of neuronal injury according to the revised National Institute on Aging–Alzheimer's Association criteria.
Objective: The objective of this multicenter prospective cohort study was to examine the value of ^{18}F-FDG-PET in predicting the development of Alzheimer's disease (AD) in patients with mild cognitive impairment (MCI).
Methods: In total, 114 patients with MCI at 9 participating institutions underwent clinical and neuropsychological examinations, MRI, and ^{18}F-FDG-PET at baseline. The cases were visually classified into predefined dementia patterns by three experts. An automated analysis for ^{18}F-FDG-PET was also performed to calculate the PET score. Subjects were followed periodically for 3 years, and progression to dementia was evaluated.

*Correspondence to: Kengo Ito, Clinical and Experimental Neuroimaging, National Center for Geriatrics and Gerontology, 7-430, Morioka-cho, Obu-shi, Aichi 474-8511, Japan. Tel.: +81 562 46 2311; Fax: +81 562 44 6596; E-mail: kito@ncgg.go.jp.

ISSN 1387-2877/15/$27.50

Results: In 47% of the patients with MCI, progression of symptoms justified the clinical diagnosis of "probable AD". The PET visual interpretation predicted conversion to AD during 3-year follow-up with an overall diagnostic accuracy of 68%. Overall diagnostic accuracy of the PET score was better than that of PET visual interpretation at all follow-up intervals, and the optimized PET score threshold revealed the best performance at the 2-year follow-up interval with an overall diagnostic accuracy of 83%, a sensitivity of 70%, and a specificity of 90%. Multivariate logistic regression analysis identified the PET score as the most significant predictive factor distinguishing AD converters from non-converters.

Conclusion: The PET score is the most statistically significant predictive factor for conversion from MCI to AD, and the diagnostic performance of the PET score is more promising for rapid converters over 2 years.

Keywords: Alzheimer's disease, cerebral glucose metabolism, ^{18}F-FDG-PET, mild cognitive impairment, prospective study

INTRODUCTION

Although an effective treatment for Alzheimer's disease (AD) has not been established, it is possible to delay the progression of symptoms with pharmacological and non-pharmacological treatments. Since pathological changes, such as senile plaques, arise more than 20 years before the manifestation of AD symptomatology, early diagnosis is required for early intervention.

Mild cognitive impairment (MCI) is a diagnostic entity used to describe abnormalities of memory function that do not fulfill the criteria for dementia [1]. MCI includes prodromal AD and other causes of dementia, as well as a form of cognitive impairment that does not progress to dementia and can disappear. Recent progress in basic research on AD and advances in *in vivo* biomarkers have led to a substantial revision of the diagnostic criteria for AD [2] to capture the full spectrum of the disease and to detect its earliest stages [3]. The revised National Institute on Aging–Alzheimer's Association criteria [4–6] suggest that accuracy in diagnosing AD can be improved with information provided by structural and biological evidence of AD pathology. Such information, if discernible at the MCI stage, may allow for differentiation of early AD from MCI owing to other causes [6].

^{18}F-FDG-PET is defined as a biomarker of neuronal injury according to the revised criteria. Studies with ^{18}F-FDG-PET have reported better diagnostic performance than other modalities in distinguishing AD-converters from non-converters in amnestic MCI patients [7–14]. Most studies have shown that the presence of AD-like hypometabolism in the posterior associative and/or posterior cingulate cortex of patients with MCI is predictive of conversion to AD within 1–3 years. However, with the exception of a few studies [11–14], the studies were conducted in relatively small groups of subjects, and follow-up times were not uniform. In this study, we report data from clinical and ^{18}F-FDG-PET assessments within a multicenter prospective cohort study of subjects with amnestic MCI (Study on Diagnosis of Early Alzheimer's Disease-Japan: SEAD-Japan). The objective of this study was to investigate the diagnostic value of ^{18}F-FDG-PET findings suggesting AD-like hypometabolism in predicting MCI conversion to AD, based on a multicenter prospective study.

METHODS

Participating subjects

Subjects with amnestic MCI were recruited between January 2006 and March 2007 and followed up annually for 3 years. Subjects were recruited from memory clinics of 9 centers specializing in AD and other dementias across Japan (Supplementary Table 1). All subjects were living independently in the community at the time of their baseline evaluation. This study was approved by the Ethics Committee at every participating institution. Each subject signed an informed consent form after the nature of the procedures had been fully explained.

All patients were free of significant underlying medical, neurological, or psychiatric illnesses. Patients were initially assessed using a neuropsychological test battery, including the Mini-Mental State Examination (MMSE), Alzheimer's Disease Assessment Scale-cognitive component-Japanese version (ADAS-J cog), Clinical Dementia Rating (CDR), Geriatric Depression Scale (GDS), Everyday Memory Check List (EMCL), and Logical Memory Subset of the Wechsler Memory Scale Revised (WMS-R LM). In accordance with the inclusion criteria, MCI patients were aged between 50 and 80 years, with an MMSE score $\geq$24, a GDS score $\leq$10, a WMS-R LM I score $\leq$13, a LM II part A and part B score (maximum = 50) $\leq$8, and a CDR memory box score equal to 0.5. Patients with formal education for less than 6 years were excluded.

^{18}F-FDG-PET

Prior to baseline ^{18}F-FDG PET scanning, all subjects fasted for at least 4 h. Intravenous administration of ^{18}F-FDG (254 ± 107 MBq) was followed by a resting period of 40–60 min in a dimly-lit and quiet room, where participants were instructed to keep their eyes open. A static scan for 10.3 ± 5.5 min was performed in 2D or 3D mode after the resting period. Attenuation was corrected by a transmission scan with segmentation for dedicated PET and by a CT scan for PET/CT. Supplementary Table 2 lists the PET and PET/CT devices and reconstruction conditions.

The ^{18}F-FDG PET images were processed with the 3-dimensional stereotactic surface projections (3D-SSP) technique to generate z-score maps, using iSSP software version 3.5 (Nihon Medi-Physics Co. Ltd., Tokyo, Japan). The normal database used for generating the z-score maps was constructed based on 50 normal subjects (31 males and 19 females, average age = 57.6 y), with 10 normal subjects each from 5 participating institutions. The healthy subjects for the normal database had no memory complaint and no history of neurologic or psychiatric disorders. The results of their neurologic examination and brain imaging examinations (MR imaging or CT) were normal, and their cognitive function was judged to be normal by experienced neurologists (MMSE score, 25–30).

PET image interpretation

Three experts, blinded to clinical information, independently assessed the reconstructed PET images, referring to the 3D-SSP z-score map and correlating with MRI to classify the images into different dementia patterns of P1-P3, P1+, and N1-N3 [15]. When evaluations of the three raters did not completely match, the cases were discussed, and a consensus reading was agreed upon.

PET score

We calculated the AD t-sum, as described in previous publications [16, 17], by using the procedure implemented as module PALZ in the PMOD software package (version 3.2; PMOD Technologies, Zurich, Switzerland). The AD t-sum indicates the severity of the metabolic decrease in those brain areas that are typically affected by AD (multimodal association cortices mostly located in the temporal and parietal lobes), including an adjustment for an age effect.

In the present study, the AD t-sum was converted into the PET score by reference to its upper limit of normal, as determined previously [16], and log transformation to approach a normal distribution of values, according to the following equation [18]: PET score = log2 {(AD t-sum/11089)+1}.

MRI

All the subjects were scanned with a 1.5 T or 3T MRI system. A T1-weighted fast field echo sequence was used. Supplementary Table 3 lists the MRI devices and reconstruction conditions. T1-weighted 3-dimensional sagittal sections of the brains were acquired and analyzed on a PC using a voxel-based specific regional analysis system for Alzheimer's disease (VSRAD® advance, Eisai Co, Ltd, Tokyo, Japan), which was developed based on the voxel-based morphometry method and is now freely available [19–23]. First, equalization of voxel sizes and linear and nonlinear transformations were performed. Next, images of gray matter, white matter, and cerebrospinal fluid were separated, and the gray matter images were standardized and smoothed onto templates by using DARTEL (Wellcome Department of Imaging Neuroscience, London, UK). By using the z-score analysis method, comparative statistical analysis of the voxels was performed for the healthy control database. The database for the healthy controls contained data from 40 men and 40 women, each aged 54–86 (mean 70.2 ± 7.3) years. In this study, the averaged positive z-score in the target volume of interest (VOI) for the medial temporal structure, including the entorhinal cortex, head to tail of the hippocampus, and amygdala was used for further analyses.

Follow-up

Patients were observed at 1-year intervals for 3 years. The CDR, MMSE, EMCL, and WMS-R-LM were re-administered at each visit. Repeat ^{18}F-FDG-PET and MRI scans were optional. The ADAS-J cog was also administered as an option in selected centers. Conversion to dementia was established when the CDR became ≥1.0. No further follow-up of patients after reaching CDR ≥1.0 was requested. AD was diagnosed in a given center when a patient fulfilled both CDR ≥1.0 and the National Institute of Neurological and Communicative Disorders–Alzheimer's Disease and Related Disorders Association's (NINCDS-ADRDA) "probable AD" criteria. The diagnosis of other causes was based on established clinical criteria for each disease, including vascular dementia (VaD) [23], dementia with Lewy bodies (DLB) [25], frontotemporal dementia (FTD) [26], and Creutzfeldt–Jacob disease [27].

Researchers (YW and YA) of the study group, who were highly experienced in evaluating dementia, finalized the clinical outcome of each case based on the submitted case report form. They were blinded as to the PET results.

Logistic regression analysis

Multivariate logistic regression analyses were used to assess whether baseline ^{18}F-FDG-PET was predictive of longitudinal clinical outcome. We estimated the odds of AD converters versus non-converters as a function of age, gender, education level, WMS-R-LM II, and PET score. Results were considered significant at $p < 0.05$. Statistical analyses were performed using SPSS (version 14.0; SPSS Inc., Chicago, IL) for Windows (Microsoft).

RESULTS

Baseline characteristics and neuropsychologic reevaluation

In total, 114 patients (64 women and 50 men; mean age, 70.8 ± 7.5) were included in the study. The mean education level was 11.5 ± 3.0 years. Of these 114 patients, 23 withdrew from the study, including 5 with no follow-up, 5 with only 1 visit, and 13 with 2 visits without conversion to dementia. Because of the uncertainty concerning their cognitive status over time, these 23 patients were excluded from the outcome analyses. Of the remaining 91 subjects, 44 patients progressed to dementia, 41 developed AD, and 3 developed non-AD dementia (FTD, DLB, and VaD) (Fig. 1). The patterns of PET images for those 3 patients were as follows: FTD patient, P2; DLB and VaD patients, P1. Since AD was the primary outcome of the study, the patients with non-AD dementia were excluded from further analyses and were not considered in the denominator for the analysis of prediction accuracy. The cumulative conversion rate over 3 years was 47%.

Demographic and neuropsychological data at the initial visit in patients who developed AD (AD-converters) and those who did not (non-converters) are shown in Table 1. At baseline, the two groups differed in the MMSE, ADAS-J cog, WMS-R-LM, and GDS scores. There was no difference observed in age, educational level, or gender distribution between these two groups.

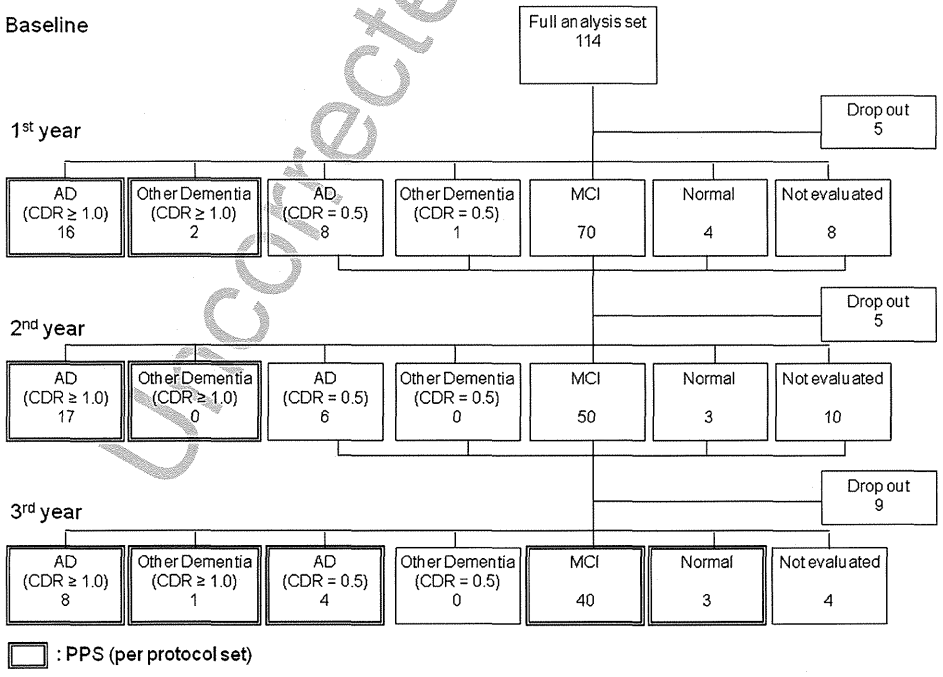

Fig. 1. Schematic summary of clinical outcomes in all MCI cases. Originally, 114 patients with MCI were included. A total of 23 patients dropped out during the 3 years. Our final sample size for the analyses of PET images was 88 patients (excluding 3 patients who converted to other dementias).

Table 1
Demographic and neuropsychological data at baseline

	AD converter (n=41) Mean (SD)	Non-converter (n=47) Mean (SD)
Age	71.2 (6.5)	70.5 (6.7)
Education (year)	12.1 (3.2)	11.8 (3.0)
WMS-R-LMI**	6.3 (3.3)	9.4 (3.2)
WMS-R-LMII**	1.7 (2.2)	4.1 (2.9)
MMSE*	25.6 (1.7)	26.9 (2.0)
ADAS*	10.6 (5.0)	7.6 (4.3)
GDS*	4.9 (2.2)	3.4 (2.0)

WMS-R-LM, Wechsler Memory Scale–Revised Logical Memory; MMSE, Mini-Mental State Examination; ADAS, Alzheimer's Disease Assessment Scale; GDS, Geriatric Depression Scale.

PET image interpretation

As the result of image interpretation, P1 and P1+ patterns were observed in 69.9% and 8.0%, respectively, and the other patterns were observed in 22.1%, including the P2 pattern in 4.4%, of all the amnestic MCI patients (Fig. 2). In this study, all P1+ cases showed a P1 pattern with occipital hypometabolism. Therefore, we combined the P1 pattern and P1+ pattern as an AD/DLB pattern for calculating the diagnostic performance.

Silverman's classification in the central image interpretation completely matched in 53% of cases, and two or more complete matches from three raters were achieved in 91% of cases. Since the P1 pattern accounted for about 70% of cases in the image interpretation, the frequency distribution of the Silverman's classification was significantly biased. A significant deviation in the distribution increases the probability of accidental match, making it difficult to correctly evaluate the degree of agreement.

The image interpretation based on the classification of PET images predicted conversion to AD during 3-year follow-up with an overall diagnostic accuracy of 68%, a sensitivity of 98%, and a specificity of 41% for the full analysis data set of the 88 subjects in this study.

The diagnostic parameters for each follow-up interval are summarized in Table 2.

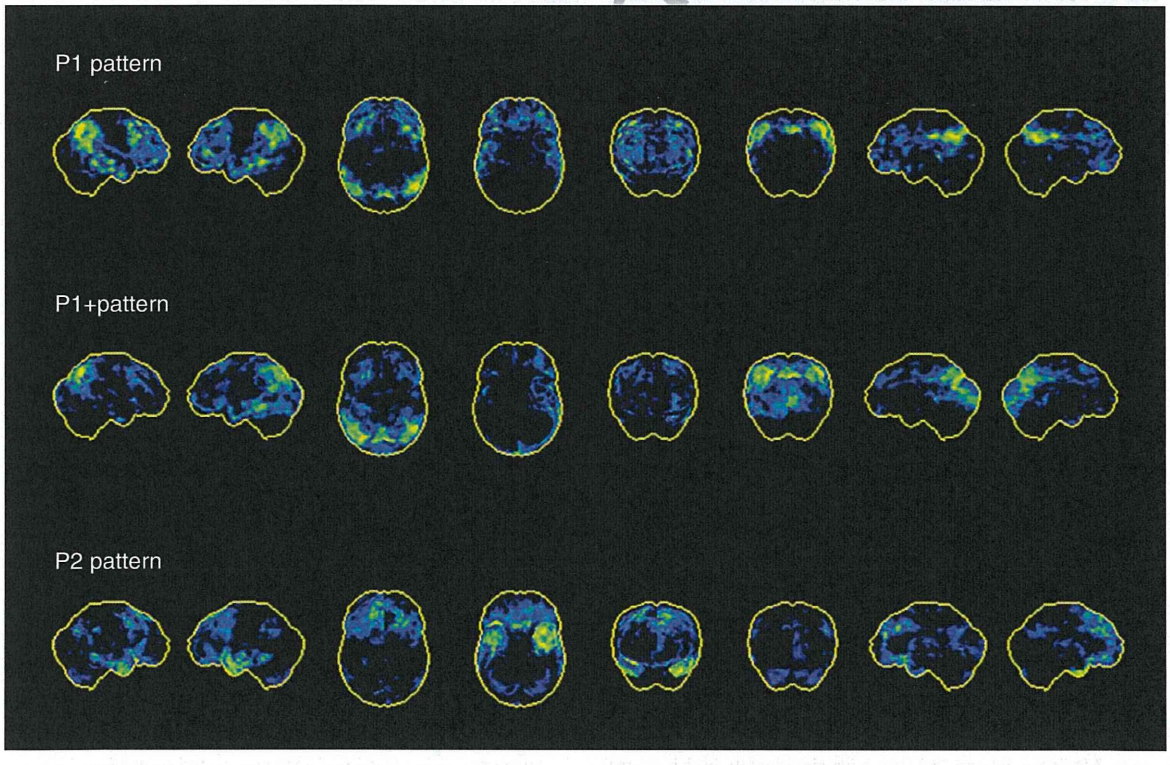

Fig. 2. 3D-SSP z-score maps showing hypometabolism in the progressive pattern groups (P1 pattern group, P1+ pattern group, and P2 pattern group) in comparison with the normal database are shown. From left to right, 3D-SSP maps are shown on the right lateral, left lateral, superior, inferior, anterior, posterior, and right and left middle views of a standardized brain image.

Table 2
Diagnostic parameters

Variable	Follow-up intervals (y)	AUC (95% CI)	Cutoff	SEN	SPE	ACC	PPV	NPV
PET visual interpretation	1	–	–	1.00	0.22	0.35	0.21	1.00
	2	–	–	0.97	0.32	0.56	0.45	0.95
	3	–	–	0.98	0.41	0.68	0.60	0.95
PET score	1	0.708 (0.569–0.846)	1.03	0.69	0.75	0.74	0.34	0.93
	2	0.809 (0.714–0.905)	1.03	0.70	0.90	0.83	0.79	0.84
	3	0.747 (0.641–0.852)	1.03	0.61	0.91	0.77	0.86	0.73
VSRAD z-score	1	0.679 (0.533–0.825)	1.47	0.75	0.57	0.60	0.26	0.92
	2	0.684 (0.570–0.799)	1.44	0.69	0.64	0.66	0.51	0.79
	3	0.658 (0.543–0.774)	1.44	0.64	0.64	0.64	0.60	0.68

AUC, area under the curve; SEN, sensitivity; SPE, specificity; ACC, accuracy; PPV, positive predictive value; NPV, negative predictive value.

PET score

The PET scores at baseline were 1.26 ± 0.69 for the AD converters and 0.70 ± 0.44 for the non-converters, respectively ($p < 0.001$). It was hypothesized that subjects who had a PET score at baseline above 1.0 had a significantly increased risk for progression. The statistics for predicting progression during 3-year follow-up were sensitivity, 61%; specificity, 79%; and accuracy, 70%. When mean PET scores were calculated according to conversion time, converters in the 1st and 2nd year showed a significantly higher PET score compared to that of non-converters. In contrast, converters in the 3rd year showed no difference in the mean PET score compared to non-converters (Fig. 3). The diagnostic accuracy during the 2-year follow-up was more promising, with an overall diagnostic accuracy of 76%, a sensitivity of 70%, and a specificity of 80%.

Area under the curve of ROC analysis for the PET score was greatest for 2-year follow-up. The ROC-derived PET score thresholds obtained using Youden index [28] yielded an adjusted accuracy of 83%, with 70% sensitivity and 90% specificity at a threshold value of PET score = 1.03 during 2-year follow-up. The diagnostic parameters for each follow-up interval are summarized in Table 2.

MRI

Because four cases at one institution were examined exceptionally with a 3T MRI system, those four were excluded from further analysis.

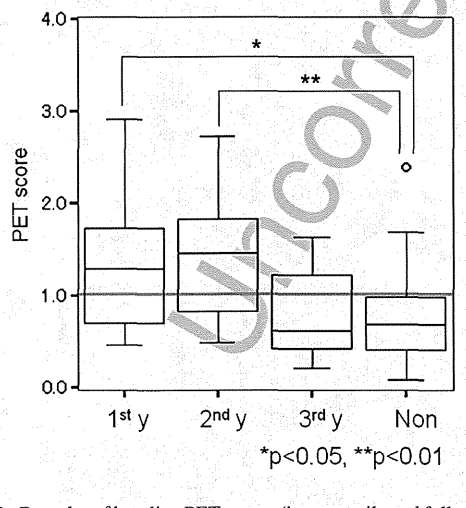

Fig. 3. Box plot of baseline PET scores (interquartile and full range) for converters according to conversion time. MCI patients progressing to AD in the 1st and 2nd year have significantly higher scores than non-converters ($p < 0.05$ and $p < 0.01$ in Tukey multiple comparisons). 1st y = 1st year converter, 2nd y = 2nd year converter, 3rd y = 3rd year converter, and Non = non-converter.

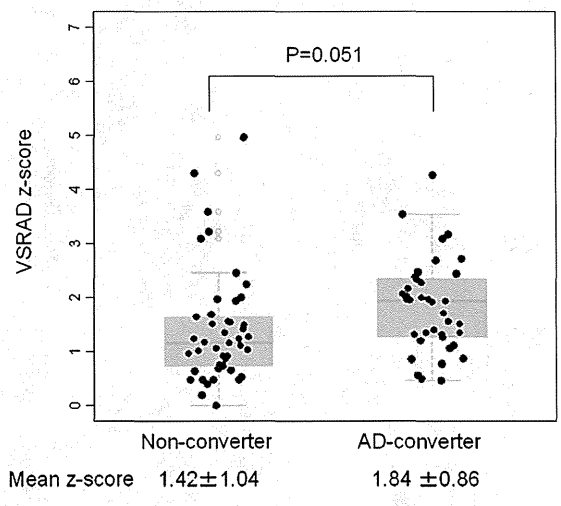

Fig. 4. Comparison between AD converters and non-converters on VSRAD z-scores in the target VOI for the left medial temporal structures. There was no significant difference between the two groups ($p = 0.051$). VSRAD, voxel-based specific regional analysis system for Alzheimer's disease.

For the AD converters and non-converters, the bilateral mean z-scores in the target VOI for the medial temporal structures at baseline were 1.84 ± 0.75 and 1.57 ± 1.01, respectively ($p = 0.191$); the right side mean z-scores were 1.80 ± 0.93 and 1.66 ± 1.13, respectively ($p = 0.543$); and the left side mean z-scores were 1.84 ± 0.86 and 1.42 ± 1.04, respectively ($p = 0.051$). Thus, the AD converters showed a tendency toward higher mean z-score in the target VOI for the left medial temporal structures but did not reach significance (Fig. 4).

Area under the curve of ROC analysis for VSRAD z-score was greatest for 2-year follow-up (Table 2). The ROC-derived thresholds using Youden index [28] for VSRAD mean z-score yielded an adjusted accuracy of 66%, with 69% sensitivity, and 64% specificity at a threshold value of VSRAD z-score = 1.44 during 2-year follow-up.

Logistic regression analysis

Multivariate logistic regression analysis identified PET score and WMS-R-LM II as predictors distinguishing AD converters from non-converters over 2 years. When age, gender, education level, WMS-R-LM II, and PET score were submitted to the forced entry procedure, AD conversion was associated significantly with the PET score ($p < 0.0001$; odds ratio, 28.25; 95% confidence interval [CI], 6.02–132.6) and WMS-R-LM II ($p = 0.001$; odds ratio, 0.61; 95% CI, 0.46–0.81) (Table 3). The combination of PET score and WMS-R-LM II distinguished AD converters from non-converters with 84.8% accuracy, 72.7% sensitivity, and 91.5% specificity.

DISCUSSION

In this study, 41 (47%) of 88 MCI patients progressed to AD. The annual conversion rate was 15.7% during the 3-year follow-up. These results are consistent with reports from other groups, indicating that, annually, 12% to 15% of amnestic MCI patients progress to AD [1].

Group comparisons based on classification of the PET image interpretations demonstrated heterogeneity in ^{18}F-FDG-PET among subjects with amnestic MCI (Fig. 2). Although the progressive pattern included the P1 pattern (69.9%), the P1+ pattern (8.0%), and the P2 pattern (4.4%), 41 (93.2%) of 44 converters were AD converters with 3 converting to DLB, FTD, and VaD.

The frequency of the P1+ pattern in the absence of DLB was relatively high. We reported that 28% of patients with AD had reduced blood flow in the occipital lobe [29]. Additionally, in our prospective SPECT study to examine the value of ^{123}I-N-Isopropyl-4-Iodoamphetamine cerebral blood flow SPECT with regard to early diagnosis of AD in patients with MCI, the frequency of the DLB pattern was 18.7% of all patients with amnestic MCI [30]. We assumed that older patients in general tend to have reduced blood flow or glucose metabolism in the occipital lobe, including those with AD. This is a topic for a future study.

Because we considered that differentiating between AD and DLB based on reduced blood flow or glucose metabolism in the occipital lobe was difficult and that PET scores do not distinguish DLB from AD, we applied pooling of the P1 pattern with the P1+ pattern in this study in the same way as in our previous SPECT study [30]. Although we analyzed the data for the P1 pattern only, the results were almost the same as those when pooling P1 with P1+(data not shown). Therefore, we believe that combining the P1 pattern with the P1+ pattern as an AD/DLB pattern to investigate the role of ^{18}F-FDG-PET in predicting conversion to AD is not problematic. The clinical significance of the heterogeneity in ^{18}F-FDG-PET should be further evaluated.

The diagnostic performance of ^{18}F-FDG-PET was calculated based on the clinical outcomes after 3 years of follow-up. The PET image interpretation showed a high sensitivity for detection of AD-converters, but its specificity was relatively low. Low specificity

Table 3
Results of multivariate logistic regression analyses for predictors of AD conversion

Variable	Coefficient (B)	SE	Wald	df	p value	Odds ratios	95% CI	
Age	0.019	0.063	0.092	1	0.761	1.019	0.901	1.153
Gender	−0.958	0.743	1.662	1	0.197	0.384	0.089	1.646
Education level	0.041	0.114	0.129	1	0.720	1.042	0.833	1.303
WMS-R-LMII	−0.502	0.146	11.887	1	0.001	0.605	0.455	0.805
PET score	3.341	0.789	17.942	1	<0.0001	28.252	6.021	132.572
Constant	−4.051	4.994	0.658	1	0.417	0.017		

df, degree of freedom; CI, confidence Interval; WMS-R-LM, Wechsler Memory Scale–Revised Logical Memory.

indicated that some non-converters showed AD/DLB-like hypometabolism on ^{18}F-FDG-PET images. These results were not in line with previous reports [7–11] where higher specificity and diagnostic accuracy were reported. The true reason for low specificity in spite of a longer follow-up compared to previous reports is unclear. One possible explanation is the difference in the characteristics of registered MCI patients for each study. In fact, conversion rates from MCI to AD were very high in some studies. Such an increase in the ratio of converters may result in a decrease in false-positive cases.

Considering the higher mean PET scores of converters in the 1st and 2nd year of follow-up, we hypothesized that the rapid converters showed more distinct AD/DLB-like hypometabolism compared to the slower converters. Although a threshold effect might exist, overall accuracy of the PET score was better than that of visual assessment at all time intervals, as shown in Table 2. As the PET score is a numerical index, PET score threshold can be optimized to maximize the prediction accuracy. The best performance of PET score was achieved at the 2-year follow-up interval. In other words, the PET score was efficient at identifying rapid converters during the 2-year follow-up.

Multivariate logistic regression analysis demonstrated that the PET score derived from ^{18}F-FDG-PET was the most significant predictor for conversion to AD among amnestic MCI patients across institutions where various types of PET or PET-CT devices were used. These results were in line with recent reports using data from the Alzheimer's Disease Neuroimaging Initiative [12–14]. Furthermore, WMS-R-LM was identified as a significant predictor for conversion to AD. A combination of statistically significant predictors, both PET score and WMS-R-LM, could assist in early stratification of patients into high- or low-risk groups.

On the other hand, the VSRAD® z-score for MRI failed to identify MRI as a predictor to distinguish AD converters from non-converters. Our results were in line with a previous study showing that ^{18}F-FDG PET is a better predictor of conversion than MR imaging [12, 14]. The possible reasons why FDG PET offers greater accuracy or sensitivity than other biomarkers at the MCI stage are not fully understood, although there is growing consensus that metabolic deficits are greater in magnitude than volumetric changes earlier in the disease.

The present study had some limitations. First, our neuropsychological test batteries were limited and did not include tests specifically designed to assess cognitive function for the early diagnosis of AD, although the MMSE and WMS-R-LM are more practical for use in a routine clinical scenario. Second, the mean age of individuals in the normal database for 3D-SSP was lesser than that of the patient group. Further analysis would be needed using an age-matched normal database. Third, although only a VBM using VSRAD® was used to evaluate volumetric changes of MRI, different methodologies such as cortical approaches rather than voxel-based approaches should be further applied [31]. Fourth, the primary outcome (conversion to AD) contained some error because some patients classified as non-converters may convert to AD with longer follow-up. Therefore, improvement of specificity and diagnostic accuracy of the PET image interpretation can be expected due to a decrease in false-positive cases provided by a longer follow-up period.

CONCLUSIONS

Visually assessed ^{18}F-FDG-PET is a very sensitive but relatively nonspecific measure for predicting conversion to AD in patients with MCI. On the other hand, the PET score is the most statistically significant predictive factor for conversion from MCI to AD, and the diagnostic performance of the PET score is more promising for rapid converters over 2 years.

ACKNOWLEDGMENTS

The authors are indebted to Professor Daniel Hillel Silverman for his valuable and constructive suggestions regarding this paper.

This work was supported by the Health Labour Sciences Research Grant from the Ministry of Health, Labour, and Welfare of Japan (H17-Tyojyu-023) and the Research Funding for Longevity Sciences from National Center for Geriatrics and Gerontology, Japan (20-1). The authors thank those people who contributed to the subjects' care and to the collection of PET images and clinical reports.

This study is registered UMIN ID: C000000297.

The funding sources had no role in study design, data collection, data analyses, or data interpretation.

Authors' disclosures available online (http://j-alz.com/manuscript-disclosures/14-1338r1).

SUPPLEMENTARY MATERIAL

The supplementary material is available in the electronic version of this article: http://dx.doi.org/10.3233/JAD-141338.

REFERENCES

[1] Petersen RC (2004) Mild cognitive impairment as a diagnostic entity. *J Intern Med* **256**, 183-194.

[2] Dubois B, Feldman HH, Jacova C, Dekosky ST, Barberger-Gateau P, Cummings J, Delacourte A, Galasko D, Gauthier S, Jicha G, Meguro K, O'brien J, Pasquier F, Robert P, Rossor M, Salloway S, Stern Y, Visser PJ, Scheltens P (2007) Research criteria for the diagnosis of Alzheimer's disease: Revising the NINCDS-ADRDA criteria. *Lancet Neurol* **6**, 734-746.

[3] Dubois B, Feldman HH, Jacova C, Cummings JL, Dekosky ST, Barberger-Gateau P, Delacourte A, Frisoni G, Fox NC, Galasko D, Gauthier S, Hampel H, Jicha GA, Meguro K, O'Brien J, Pasquier F, Robert P, Rossor M, Salloway S, Sarazin M, de Souza LC, Stern Y, Visser PJ, Scheltens P (2010) Revising the definition of Alzheimer's disease: A new lexicon. *Lancet Neurol* **9**, 1118-1127.

[4] Albert MS, DeKosky ST, Dickson D, Dubois B, Feldman HH, Fox NC, Gamst A, Holtzman DM, Jagust WJ, Petersen RC, Snyder PJ, Carrillo MC, Thies B, Phelps CH (2011) The diagnosis of mild cognitive impairment due to Alzheimer's disease: Recommendations from the National Institute on Aging-Alzheimer's Association workgroups on diagnostic guidelines for Alzheimer's disease. *Alzheimers Dement* **7**, 270-279.

[5] Sperling RA, Aisen PS, Beckett LA, Bennett DA, Craft S, Fagan AM, Iwatsubo T, Jack CR Jr, Kaye J, Montine TJ, Park DC, Reiman EM, Rowe CC, Siemers E, Stern Y, Yaffe K, Carrillo MC, Thies B, Morrison-Bogorad M, Wagster MV, Phelps CH (2011) Toward defining the preclinical stages of Alzheimer's disease: Recommendations from the National Institute on Aging-Alzheimer's Association workgroups on diagnostic guidelines for Alzheimer's disease. *Alzheimers Dement* **7**, 280-292.

[6] McKhann GM, Knopman DS, Chertkow H, Hyman BT, Jack CR Jr, Kawas CH, Klunk WE, Koroshetz WJ, Manly JJ, Mayeux R, Mohs RC, Morris JC, Rossor MN, Scheltens P, Carrillo MC, Thies B, Weintraub S, Phelps CH (2011) The diagnosis of dementia due to Alzheimer's disease: Recommendations from the National Institute on Aging-Alzheimer's Association workgroups on diagnostic guidelines for Alzheimer's disease. *Alzheimers Dement* **7**, 263-269.

[7] Anchisi D, Borroni B, Franceschi M, Kerrouche N, Kalbe E, Beuthien-Beumann B, Cappa S, Lenz O, Ludecke S, Marcone A, Mielke R, Ortelli P, Padovani A, Pelati O, Pupi A, Scarpini E, Weisenbach S, Herholz K, Salmon E, Holthoff V, Sorbi S, Fazio F, Perani D (2005) Heterogeneity of brain glucose metabolism in mild cognitive impairment and clinical progression to Alzheimer disease. *Arch Neurol* **62**, 1728-1733.

[8] Arnaiz E, Jelic V, Almkvist O, Wahlund LO, Winblad B, Valind S, Nordberg A (2001) Impaired cerebral glucose metabolism and cognitive functioning predict deterioration in mild cognitive impairment. *Neuroreport* **12**, 851-855.

[9] Mosconi L, Perani D, Sorbi S, Herholz K, Nacmias B, Holthoff V, Salmon E, Baron JC, De Cristofaro MT, Padovani A, Borroni B, Franceschi M, Bracco L, Pupi A (2004) MCI conversion to dementia and the APOE genotype: A prediction study with FDG-PET. *Neurology* **63**, 2332-2340.

[10] Drzezga A, Grimmer T, Riemenschneider M, Lautenschlager N, Siebner H, Alexopoulus P, Minoshima S, Schwaiger M, Kurz A (2005) Prediction of individual clinical outcome in MCI by means of genetic assessment and (18)F-FDG PET. *J Nucl Med* **46**, 1625-1632.

[11] Silverman DHS, Truong CT, Kim SK, Chang CY, Chen W, Kowell AP, Cummings JL, Czernin J, Small GW, Phelps ME (2003) Prognostic value of regional cerebral metabolism in patients undergoing dementia evaluation: Comparison to a quantifying parameter of subsequent cognitive performance and to prognostic assessment without PET. *Mol Genet Metab* **80**, 350-355.

[12] Landau SM, Harvey D, Madison CM, Reiman EM, Foster NL, Aisen PS, Petersen RC, Shaw LM, Trojanowski JQ, Jack CR Jr, Weiner MW, Jagust WJ (2010) Alzheimer's Disease Neuroimaging Initiative. Comparing predictors of conversion and decline in mild cognitive impairment. *Neurology* **75**, 230-238.

[13] Chen K, Ayutyanont N, Langbaum JBS, Fleisher AS, Reschke C, Lee W, Liu X, Bandy D, Alexander GE, Thompson PM, Shaw L, Trojanowski JQ, Jack CR Jr, Landau SM, Foster NL, Harvey DJ, Weiner MW, Koeppe RA, Jagust WJ, Reiman EM (2011) Alzheimer's Disease Neuroimaging Initiative. Characterizing Alzheimer's disease using a hypometabolic convergence index. *Neuroimage* **56**, 52-60.

[14] Shaffer JL, Petrella JR, Sheldon FC, Choudhury KR, Calhoun VD, Coleman RE, Doraiswamy PM (2013) Alzheimer's Disease Neuroimaging Initiative. Predicting cognitive decline in subjects at risk for Alzheimer disease by using combined cerebrospinal fluid, MR imaging, and PET biomarkers. *Radiology* **266**, 583-591.

[15] Silverman DH, Small GW, Chang CY, Lu CS, Kung De Aburto MA, Chen W, Czernin J, Rapoport SI, Pietrini P, Alexander GE, Schapiro MB, Jagust WJ, Hoffman JM, Welsh-Bohmer KA, Alavi A, Clark CM, Salmon E, de Leon MJ, Mielke R, Cummings JL, Kowell AP, Gambhir SS, Hoh CK, Phelps ME (2001) Positron emission tomography in evaluation of dementia: Regional brain metabolism and long-term outcome. *JAMA* **286**, 2120-2127.

[16] Herholz K, Salmon E, Perani D, Baron JC, Holthoff V, Frölich L, Schönknecht P, Ito K, Mielke R, Kalbe E, Zündorf G, Delbeuck X, Pelati O, Anchisi D, Fazio F, Kerrouche N, Desgranges B, Eustache F, Beuthien-Baumann B, Menzel C, Schröder J, Kato T, Arahata Y, Henze M, Heiss WD (2002) Discrimination between Alzheimer dementia and controls by automated analysis of multicenter FDG PET. *Neuroimage* **17**, 302-316.

[17] Haense C, Herholz K, Jagust WJ, Heiss WD (2009) Performance of FDG PET for detection of Alzheimer's disease in two independent multicenter samples (NEST-DD and ADNI). *Dement Geriatr Cogn Disord* **28**, 259-266.

[18] Herholz K, Westwood S, Haense C, Dunn G (2011) Evaluation of a calibrated (18)F-FDG PET score as a biomarker for progression in Alzheimer disease and mild cognitive impairment. *J Nucl Med* **52**, 1218-1226.

[19] Hirata Y, Matsuda H, Nemoto K, Ohnishi T, Hirao K, Yamashita F, Asada T, Iwabuchi S, Samejima H (2005) Voxel-based morphometry to discriminate early Alzheimer's disease from controls. *Neurosci Lett* **382**, 269-274.

[20] Matsuda H (2007) Role of neuroimaging in Alzheimer's disease, with emphasis on brain perfusion SPECT. *J Nucl Med* **48**, 1289-1300.

[21] Matsuda 21, H (2007) The role of neuroimaging in mild cognitive impairment. *Neuropathology* **27**, 570-577.

[22] Niida R, Niida A, Motomura M, Uechi A (2011) Diagnosis of depression by MRI scans with the use of VSRAD-a promising auxiliary means of diagnosis: A report of 10 years research. *Int J Gen Med* **4**, 377-387.

[23] Matsuda H, Mizumura S, Nemoto K, Yamashita F, Imabayashi E, Sato N, Asada T (2012) Automatic voxel-based morphometry of structural MRI by SPM8 plus diffeomorphic anatomic

registration through exponentiated lie algebra improves the diagnosis of probable Alzheimer disease. *AJNR Am J Neuroradiol* **33**, 1109-1114.

[24] Roman GC, Tatemichi TK, Erkinjuntti T, Cummings JL, Masdeu JC, Garcia JH, Amaducci L, Orgogozo JM, Brun A, Hofman A, Moody DM, O'Brien MD, Yamaguchi T, Grafman J, Drayer BP, Bennett DA, Fisher M, Ogata J, Kokmen E, Bermejo F, Wolf PA, Gorelick PB, Bick KL, Pajeau AK, Bell MA, DeCarli C, Culebras A, Korczyn AD, Bogousslavsky J, Hartmann A, Scheinberg P (1993) Vascular dementia: Diagnostic criteria for research studies-report of the NINDS-AIRENS International Workshop. *Neurology* **43**, 250-260.

[25] McKeith IG, Galasko D, Kosaka K, Perry EK, Dickson DW, Hansen LA, Salmon DP, Lowe J, Mirra SS, Byrne EJ, Lennox G, Quinn NP, Edwardson JA, Ince PG, Bergeron C, Burns A, Miller BL, Lovestone S, Collerton D, Jansen EN, Ballard C, de Vos RA, Wilcock GK, Jellinger KA, Perry RH (1996) Consensus guidelines for the clinical and pathologic diagnosis of dementia with Lewy bodies (DLB): Report of the Consortium on DLB International Workshop. *Neurology* **47**, 1113-1124.

[26] McKhann G, Albert MS, Grossman M, Miller B, Dickson D, Trojanowski JQ (2001) Clinical and pathological diagnosis of frontotemporal dementia. *Ann Neurol* **58**, 1803-1809.

[27] Knopman DS, DeKosky ST, Cummings JL, Chui H, Corey-Bloom J, Relkin N, Small GW, Miller B, Stevens JC (2001) Practice parameter: Diagnosis of dementia (an evidence-based review). Report of the Quality Standards Subcommittee of the American Academy of Neurology. *Neurology* **56**, 1143-1153.

[28] Youden WJ (1950) Index for rating diagnostic tests. *Cancer* **3**, 32-35.

[29] Ishii K, Ito K, Nakanishi A, Kitamura S, Terashima A (2014) Computer-assisted system for diagnosing degenerative dementia using cerebral blood flow SPECT and 3D-SSP: A multicenter study. *Jpn J Radiol* **32**, 383-390.

[30] Ito K, Mori E, Fukuyama H, Ishii K, Washimi Y, Asada T, Mori S, Meguro K, Kitamura S, Hanyu H, Nakano S, Matsuda H, Kuwabara Y, Hashikawa K, Momose T, Uchida Y, Hatazawa J, Minoshima S, Kosaka K, Yamada T, Yonekura Y, Study J-COSMIC, Group (2013) Prediction of outcomes in MCI with (123)I-IMP-CBF SPECT: A multicenter prospective cohort study. *Ann Nucl Med* **27**, 898-906.

[31] Cuingnet R, Gerardin E, Tessieras J, Auzias G, Lehericy S, Habert MO, Chupin M, Benali H, Colliot O (2010) Alzheimer's Disease Neuroimaging Initiative. Automatic classification of patients with Alzheimer's disease from structural MRI: A comparison of ten methods using the ADNI database. *Neuroimage* **56**, 766-781.

Jpn J Radiol (2014) 32:383–390
DOI 10.1007/s11604-014-0329-6

ORIGINAL ARTICLE

Computer-assisted system for diagnosing degenerative dementia using cerebral blood flow SPECT and 3D-SSP: a multicenter study

Kazunari Ishii · Kengo Ito · Atsushi Nakanishi · Shin Kitamura · Akira Terashima

Received: 10 January 2014 / Accepted: 16 April 2014 / Published online: 17 May 2014

Abstract
Purpose Due to increasing numbers of patients with dementia, more physicians who do not specialize in brain nuclear medicine are being asked to interpret SPECT images of cerebral blood flow. We conducted a multicenter study to determine whether a computer-assisted diagnostic system *Z*-score summation analysis method (ZSAM) using three-dimensional stereotactic surface projections (3D-SSP) can differentiate Alzheimer's disease (AD)/dementia with Lewy bodies (DLB) and non-AD/DLB in institutions using various types of gamma cameras.
Method We determined the normal thresholds of *Z*-sum (summed *Z*-score) within a template region of interest for each single photon emission computed tomography (SPECT) device and then compared them with the *Z*-sums of patients and calculated the accuracy of the differential diagnosis by ZSAM. We compared the diagnostic accuracy between ZSAM and visual assessment.
Patients We enrolled 202 patients with AD (mean age, 76.8 years), 40 with DLB (mean age 76.3 years) and 36 with non-AD/DLB (progressive supranuclear palsy, $n = 10$; frontotemporal dementia, $n = 20$; slowly progressive aphasia, $n = 2$ and one each with idiopathic normal pressure hydrocephalus, corticobasal degeneration, multiple system atrophy and Parkinson's disease) who underwent *N*-isopropyl-*p*-[^{123}I] iodoamphetamine cerebral blood flow SPECT imaging at each participating institution.
Results The ZSAM sensitivity to differentiate between AD/DLB and non-AD/DLB in all patients, as well as those with mini-mental state examination scores of ≥24 and 20–23 points were 88.0, 78.0 and 88.4 %, respectively, with specificity of 50.0, 44.4 and 60.0 %, respectively. The diagnostic accuracy rates were 83.1, 72.9 and 84.2 %, respectively. The areas under receiver operating characteristics curves for visual inspection by four expert raters were 0.74–0.84, 0.66–0.85 and 0.81–0.93, respectively, in the same patient groups. The diagnostic accuracy rates were 70.9–89.2 %, 50.9–84.8 % and 76.2–93.1 %, respectively.
Conclusion The diagnostic accuracy of ZSAM to differentiate AD/DLB from other types of dementia or degenerative diseases regardless of severity was equal to that of visual assessment by expert raters even across several institutions. These findings suggested that ZSAM could serve as a supplementary tool to help expert evaluators who differentially diagnose dementia from SPECT images by visual assessment.

Keywords Alzheimer's disease · Lewy bodies · Cerebral blood flow · *Z*-score summation analysis · Dementia

K. Ishii (✉)
Department of Radiology, Faculty of Medicine, Kinki University, 377-2 Osakasayama, Osaka 589-8511, Japan
e-mail: kishii@hbhc.jp; ishii@med.kindai.ac.jp

K. Ito
Department of Clinical and Experimental Neuroimaging, Center for Development of Advanced Medicine for Dementia, National Center for Geriatrics and Gerontology, Obu, Aichi, Japan

A. Nakanishi
Department of Radiology, School of Medicine, Juntendo University, Tokyo, Japan

S. Kitamura
Department of Internal Medicine, Nippon Medical School Musashi Kosugi Hospital, Kawasaki, Kanagawa, Japan

A. Terashima
Institute for Aging Brain and Cognitive Disorders, Hyogo Brain and Heart Center, Himeji, Hyogo, Japan

Introduction

Society is rapidly aging, and the increase in the numbers of patients with dementia is posing considerable medical and social problems. Alzheimer's disease (AD) is the most common degenerative dementia, and it can be diagnosed by functional brain imaging using fluorodeoxyglucose (FDG) positron emission tomography (PET) and SPECT [1, 2]. Although PET can diagnostically differentiate AD more precisely than SPECT, PET costs are not covered by insurance in many European countries and in Japan. Thus, FDG-PET is not used in the medical care of patients with dementia, and cerebral blood flow SPECT is exclusively used because it is covered by insurance. As the number of patients with dementia has increased, physicians who are not specialists in cerebral nuclear medicine are often obliged to interpret cerebral blood flow SPECT images. Atypical findings are obvious on cerebral blood flow SPECT images of dementia, but subtle differences can be difficult even for experts in brain nuclear medicine to diagnose. On the other hand, a statistical image analysis provides a tangible result, since it is determined based on specific criteria. A computer-assisted diagnostic system has shown promise as a supplementary measure for interpreting cerebral blood flow SPECT images [3]. We conducted a multicenter study to determine its applicability.

Patients and methods

Procedure

The analysis *Z*-score summation analysis method (ZSAM) using the computer-assisted diagnostic system as described [3] comprises the following procedures.

1. The IMP-SPECT images of normal individuals are analyzed using 3D-SSP [4] to generate *Z*-score images. *Z*-scores are calculated using the following formula: *Z*-score = ([normal mean] − [individual value])/(normal standard deviation). Summed positive *Z*-scores (*Z*-sum) are obtained from template ROIs (parietal lobe, posterior cingulate gyrus and precuneus, medial surface of the occipital lobe and the lateral surface of the occipital lobe) that are regions of characteristic blood flow reduction in *Z*-score images of AD and DLB. This is because each ROI includes negative and positive *Z*-scores and reduced blood flow appears as a positive *Z*-score.
2. The *Z*-sum of some normal individuals is averaged for each ROI and the normal threshold of the *Z*-sum with the mean value and standard deviation is calculated.
3. The *Z*-sum of patients processed by the same procedure as (1) is compared with the normal threshold calculated above in (2).
4. Blood flow is considered to be reduced if the *Z*-sum of the patient exceeds the normal threshold.

Various SPECT devices are used for cerebral blood flow SPECT, and a normal database that conforms to each SPECT device is used in 3D-SSP analysis. This multicenter study determines whether AD/DLB can be differentiated from other types of dementia and degenerative diseases using new template ROIs and the normal thresholds of the *Z*-sum set for each normal database.

Patients

The study proceeded according to the clinical study guidelines of each institution and was approved by each independent ethics committee.

Preparation of template ROIs (group 1)

We prepared template ROIs from 36 patients with probable AD and 13 with probable dementia with Lewy bodies (DLB) who underwent cerebral blood flow SPECT with IMP using a Siemens e.cam at the Hyogo Brain and Heart Center between August and December in 2008. We used the diagnostic criteria of the Neurological and Communicative Disorders and Stroke-Alzheimer's Disease and Related Disorders Association (NINCDS/ADRDA) for AD [5] and those of the third report of the Dementia with Lewy Bodies Consortium for DLB [6]. Patients with cerebrovascular disease were excluded in this study. A normal database created from 29 normal volunteers specifically prepared for the Siemens e.cam by Onishi et al. [7] served as the comparative group. The patients in the AD, DLB and normal database groups were 78.1 ± 6.4, 75.9 ± 6.6, and 64.2 ± 8.2 years old, respectively, and the MMSE scores of the AD and DLB groups were 20.7 ± 3.8 and 19.4 ± 7.4 points, respectively.

Diagnostic performance review (group 2)

The diagnostic performance of ZSAM was determined based on data from 202 patients diagnosed with probable AD according to the NINCDS-ADRDA diagnostic criteria [5], 40 diagnosed with probable DLB based on the third report of the DLB Consortium diagnostic criteria [6], 20 with FTD who met FTD diagnostic criteria [8], 10 with PSP who met the National Institute of Neurological Disorders and the Society for Progressive Supranuclear Palsy (NINDS-SPSP) International Workshop diagnostic criteria [9], two with slowly-progressive

aphasia, and one each with iNPH, CBD, MSA and PD who presented at the medical institutions involved in this study between December 2007 and February 2011. The slowly progressive aphasia (SPA), iNPH, CBD, MSA, and PD were diagnosed according to disease-specific criteria [10–13]. The mean ± SD of age (years) and MMSE scores for AD, DLB, FTD, PSP and SPA were 76.8 ± 7.2 and 19.4 ± 4.7, 76.3 ± 5.7 and 20.2 ± 5.0, 70.6 ± 9.0 and 20.1 ± 5.5, 71.6 ± 6.6 and 21.6 ± 4.6, and 64.5 ± 1.5 and 21.0 ± 1.0, respectively. The age (years) and MMSE scores for those with iNPH, CBD, MSA and PD were 76 and 17, 64 and 23, 82 and 22, and 83 and 23, respectively. Both AD and DLB were included in the AD/DLB group, and FTD, PSP, SPA, iNPH, CBD, MSA, and PD were included in the non-AD/DLB group. We selected patients with MMSE scores of ≥24 and 20–23 points to determine the diagnostic accuracy of ZSAM for mild disease (Table 1).

Table 1 Demographic data of the subjects

Group	Number	Age (years)	MMSE (score)
First Group			
AD	36	78.1±6.4	20.7±3.8
DLB	13	75.9±6.6	19.4±7.4
Second Group all			
AD/DLB_group			
AD	202	76.8±7.2	19.4±4.7
DLB	40	76.3±5.7	20.2±5.0
nonAD/nonDLB_group	36	71.1±8.4	20.7±4.9
Second Group MMSE 24 and more			
AD/DLB_group			
AD	40	75.3±6.3	25.4±1.6
DLB	10	73.0±6.8	25.6±1.3
nonAD/nonDLB_group	9	69.3±6.6	26.0±1.5
Second Group MMSE 20-23			
AD/DLB_group			
AD	72	77.2±6.6	21.3±1.1
DLB	14	77.1±4.5	22.1±1.0
nonAD/nonDLB_group	15	72.6±9.2	22.1±0.9

SPECT image acquisition and processing

Imaging was started in the resting state 15 min after an injection of 111–222 MBq (3–6 mCi) of IMP. Table 2 lists the SPECT equipment and reconstruction conditions.

Creation of new template ROI maps

We performed stereotactic anatomic standardization as follows. The original IMP-SPECT image data were transformed into standard Talairach space using the NEUROSTAT program [4], which is the basis of 3D-SSP (Satoshi Minoshima, Department of Radiology and Bioengineering, University of Washington, Seattle, WA, USA). Detailed procedure of 3D-SSP and this program is described in the previous literature [3]. In this study, we used pixel values of individual surface maps normalized to values for mean activity in the whole brain. As a new AD/DLB template ROI map, pixels with significantly decreased perfusion in the AD group ($p < 0.05$), obtained from a comparison between the SIEMENS e.cam normal database and the AD group (first group) were plotted (Fig. 1), and as an occipital template ROI map, pixels with significantly decreased perfusion in the DLB group ($p < 0.05$), obtained from a comparison between the AD and DLB groups (first group) were plotted (Fig. 1). To create an ROI template with significantly decreased symmetrical areas in this map, larger areas than the opposite sides were set to make both sides the same size, which increased detection sensitivity in a brain with AD.

Threshold values of summed positive *Z*-scores

We calculated the threshold *Z*-sum in the new template ROI maps for diagnosis using the following jackknife-type technique. First, one patient from the normal group was selected to constitute a normal database and another normal database was prepared from the remainder of the normal group. The normal database constructed based on data from the selected normal patient was analyzed with 3D-SSP to prepare a *Z*-score image. The procedure was repeated for each patient in the normal database. The AD/DLB and occipital template ROI were set in the *Z*-score images of

Table 2 Characteristics of the SPECT study and normal database (NDB) at each institute

Institution	Camera type	Prefilter	Collimator	Cutoff frequency	Scatter correction	Attenuation correction	Matrix size	Pixel size (mm)
A	TOSHIBA GCA9300	Butterworth	LESHR-Fanbeam	0.08 cycles/pixel	TEW	Chang	128 × 128	1.72
B	TOSHIBA ECAM	Butterworth	LMEGP	0.45 cycles/pixel	non	Chang	128 × 128	3.9
C	SIEMENS e.cam	Butterworth	LMEGP	0.40 Nyquist	MEW	Chang	128 × 128	3.9
D	SIEMENS e.cam	Butterworth	LMEGP	0.45 Nyquist	MEW	Chang	128 × 128	3.9

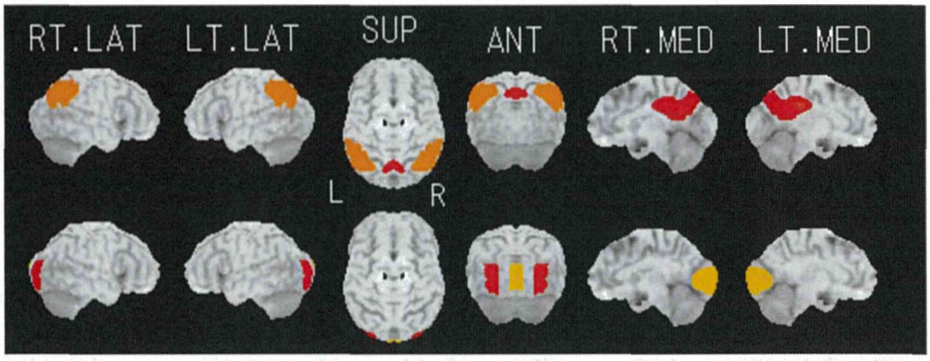

Fig. 1 Template ROI map for AD and DLB patients, which demonstrates significantly lower perfusion in AD patients compared with normal controls and DLB patients. ZSAM used this ROI map (*RT.LAT* right lateral, *LT.LAT* left lateral, *SUP* superior, *INF* inferior, *ANT* anterior, *POST* posterior, *RT.MED* right medial, *LT.MED* left medial)

Table 3 Details of healthy volunteers in NDB

Institution	Number	Age (years) mean ± SD
A	29	64.6 ± 8.4
B	27	63.4 ± 7.1
C	29	64.2 ± 8.2
D	29	64.2 ± 8.2

the normal patients to calculate the *Z*-sum for each ROI. The *Z*-sum of each normal individual was averaged for each ROI to calculate the normal mean and standard deviation of the *Z*-sum. Normal means + 1.64 SD and + 1.96 SD were considered normal *Z*-sum thresholds, and we determined that blood flow was reduced when the *Z*-sum of an analyzed individual exceeded the normal threshold. We used the normal database described by Onishi et al. [7] to prepare normal *Z*-sum thresholds (Table 3).

Clinical adoption of automated system

After preparing *Z*-score images using the normal database described above in which the reconstruction conditions were consistent with the SPECT device, we calculated the *Z*-sum within the template ROIs and compared the SPECT images of patients with the normal *Z*-sum threshold. We compared the ratios (%) of patients with AD and DLB who had reduced blood flow within each ROI. In order to make the best criteria for discriminating AD/DLB from non-AD/DLB, we established two determination criteria for AD/DLB and non-AD/DLB and determined sensitivity, specificity, and diagnostic accuracy rates for each criterion: (1) *Determination of criterion 1 for AD/DLB*. When the *Z*-sum exceeded the normal threshold in one or more of four AD/DLB template ROIs in the bilateral parietal lobe, bilateral posterior cingulate gyrus and precuneus, the patient was assigned to the AD/DLB group. Otherwise, patients were assigned to the non-AD/DLB group; (2) *Determination criterion 2 for AD/DLB*. When the *Z*-sum exceeded the normal threshold in one or more ROIs in the posterior cingulate gyrus and precuneus ROIs, or the *Z*-sum exceeded the normal threshold in two or more of four AD/DLB template ROIs, the patient was assigned to the AD/DLB group. Otherwise, patients were assigned to the non-AD/DLB group.

Diagnostic performance of conventional IMP-SPECT and 3D-SSP Z-score images

We compared automated assessments of conventional IMP-SPECT axial and 3D-SSP *Z*-score images with visual assessments by three experienced nuclear medicine physicians and one neurologist. All of them knew the criteria for abnormalities, but were blinded to the clinical data of the patients. The criteria for AD comprised decreased parietotemporal perfusion compared with sensorimotor perfusion, or obviously decreased posterior cingulate and/or precuneus perfusion compared with sensorimotor perfusion. The criterion for DLB was decreased medial and/or lateral occipital perfusion compared with sensorimotor perfusion. Diagnoses of AD/DLB vs non-AD/DLB based on the conventional IMP-SPECT and 3D-SSP *Z*-score images were classified as follows: definite non-AD/DLB, probable non-AD/DLB, indeterminate, probable AD/DLB and definite AD/DLB.

Visual assessments were evaluated using ROC analysis and AUC were calculated using IBM SPSS statistics. We then compared the diagnostic accuracy between AD/DLB and non-AD/DLB differentiated by visual assessment and ZSAM.

Results

Diagnostic accuracy between AD/DLB and non-AD/DLB differentiated by visual assessment and ZSAM

Table 4 shows the diagnostic accuracy rates of AD/DLB determination criterion 2 at a normal *Z*-sum threshold of the normal mean + 1.64 SD at which specificity between

Table 4 Comparison of the accuracy of visual inspection and ZSAM

Group	Observer	Accuracy		
		Visual inspection	ZSAM	McNemar test
All	A	89.21	83.1	$p = 0.028$
	B	77.34		NS
	C	78.78		NS
	D	70.86		$p = 0.001$
MMSE 24 and more	A	84.75	72.9	NS
	B	55.93		NS
	C	61.02		NS
	D	50.85		$p = 0.007$
MMSE 20–23	A	93.07	84.2	$p = 0.063$
	B	82.18		NS
	C	84.16		NS
	D	76.24		NS

ZSAM's criteria was set as #2 with threshold of mean + 1.64 SD

Table 5 Number of cases exceeding the Z-sum threshold in AD/DLB ROI

	Threshold	
	Mean + 1.64 SD	Mean + 1.96 SD
Parietal ROI[a]		
AD ($n = 202$)	159 (78.7 %)	146 (72.3 %)
DLB ($n = 40$)	33 (82.5 %)	31 (77.5 %)
Posterior cingulate and precuneus ROI[a]		
AD ($n = 202$)	175 (86.6 %)	166 (82.2 %)
DLB ($n = 40$)	32 (80.0 %)	30 (75.0 %)
Occipital ROI		
AD ($n = 202$)	58 (28.7 %)**	50 (24.8 %)**
DLB ($n = 40$)	24 (60 %)*	20 (50 %)**

* $p = 0.0013$, ** $p < 0.0001$ by χ^2 test

[a] There is no significant group difference by χ^2 test

determination by ZSAM and visual inspection was high. The diagnostic accuracy rates did not significantly differ between ZSAM and visual assessments by two of the four raters (McNemar test). One rater had a significantly higher visual diagnostic accuracy rate when all patients and the group with MMSE scores of 20–23 points were included. Another had a significantly higher diagnostic accuracy rate by ZSAM when all patients and those with mild disease were included.

Table 5 shows the ratios (%) of patients with reduced blood flow in the parietal lobe, posterior cingulate gyrus and precuneus and occipital lobe ROIs among 202 patients with AD and 40 patients with DLB. At a normal threshold of mean + 1.64 SD, 78.7 and 82.5 % of patients with AD and DLB, respectively, had reduced blood flow in the parietal lobe ROI, and 86.6 and 80.0 %, respectively, had reduced blood flow in the posterior cingulate gyrus and precuneus ROI. The ratios of patients with AD and DLB and reduced blood flow did not significantly differ. At normal thresholds of mean + 1.64 SD and mean + 1.96 SD, 60.0 and 50.0 % of patients, respectively, with DLB and 28.7 and 24.8 %, respectively, of those with AD had reduced blood flow in the occipital lobe ROI, with DLB being significantly higher for both situations ($p < 0.0001$, $p = 0.013$ χ^2 test).

Figure 2 shows the diagnostic performance of ZSAM (Fig. 2a) and visual assessment (Fig. 2b) for differentiating AD/DLB from non-AD/DLB. The sensitivity of ZSAM based on the AUC for all patients, and those with MMSE scores of ≥24 and 20–23 points was 85.1–93.0 %, 74.0–88.0 % and 88.4–94.2 %, respectively, with 25.0–50.0 %, 33.3–44.4 % and 33.3–60.0 %, specificity, respectively. Diagnostic accuracy rates were 80.6–84.2 %, 69.5–79.7 %, and 82.2–85.1 %, respectively.

The sensitivity of visual assessment by the four raters for all patients, and those with MMSE scores of ≥24 and 20–23 points was 71.1–94.6 %, 46.0–90.0 % and 75.6–96.5 %, respectively with 38.9–69.4 %, 22.2–77.8 % and 53.3–80.0 %, specificity, respectively. Diagnostic accuracy rates were 70.9–89.2 %, 50.6–84.8 % and 76.2–93.1 %, respectively. The AUC in the ROC analyses were 0.74–0.84, 0.66–0.85 and 0.81–0.93, respectively.

Discussion

Differentiation between AD/DLB and non-AD/DLB

Blood flow is reduced in the temporoparietal association area, posterior cingulate gyrus, and precuneus of patients with DLB as in AD, but blood flow in the occipital lobe is lower in DLB [14]. Thus, AD is impossible to differentiate from DLB in the temporoparietal association area, posterior cingulate gyrus and precuneus. To discriminate AD or DLB patients from other disease patients is the first step of differential diagnosis process. Because both in AD and DLB brain, bilateral parietal and posterior cingulate perfusion reduction exists, and in non-AD/DLB brain those regional perfusion reductions exist a minimum. After this process, we can move to discriminate AD from DLB. Therefore, patients with AD/DLB and patients with other degenerative dementias should be initially differentiated using these regions. The present study found that high ratios of patients with AD and DLB had reduced blood flow in the AD/DLB template ROIs (bilateral parietal lobe, posterior cingulate gyrus and precuneus), and that the ratios did not significantly differ. We used SPECT images of AD and normal groups to prepare AD/DLB template ROIs, but

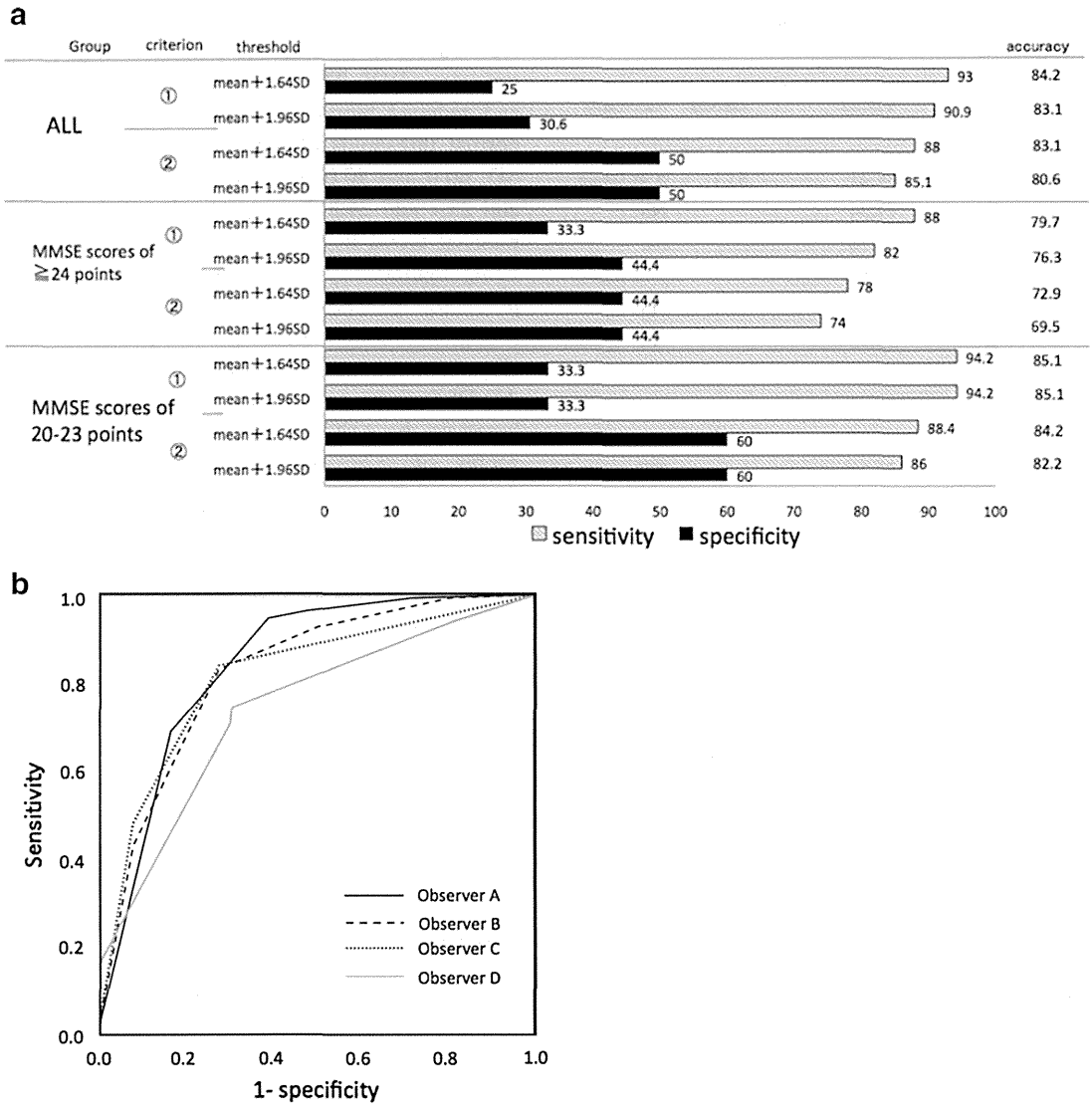

Fig. 2 **a** Graph of sensitivity, specificity and accuracy of differential diagnosis performance of ZSAM comparisons between the AD/DLB group and non-AD/non-DLB. **b** ROC curve of visual inspection of AD/DLB group vs non-AD/non-DLB

not those of the DLB group. We believe that using the ROIs as regions with which to evaluate the reduced blood flow sites characteristic of AD and DLB is not problematic.

Differentiation between AD and DLB

Although significantly more patients with DLB had reduced blood flow in the occipital lobe ROI, the ratio of 60 % was not considered very high, and 28 % of patients with AD had reduced blood flow in the occipital lobe. We assumed that older patients in general tend to have decreased perfusion in the occipital lobe, including those with AD. Because we considered that differentiating between AD and DLB based on reduced blood flow in the occipital lobe ROI was difficult, we differentiated AD/DLB from non-AD/DLB using AD/DLB template ROIs. Differentiation between AD and DLB should be improved by using not only the occipital lobe ROI but also other reference sites or clinical psychological test trials. This is a topic for a future study.

Differentiation by ZSAM

The sensitivity of for detecting AD/DLB using ZSAM was 74–88 % among patients with mild disease and MMSE scores of ≥24 points, and 88.4–94.2 % for those with MMSE scores of 20–23 points, but the specificity was low. Specificity of ZSAM was less than 60 % in contrast with sensitivity more than 70 %. High sensitivity is not useful for ruling in disease, but a high sensitivity test is reliable

when its result is negative, since it rarely misdiagnoses those AD/DLB diseases. Minoshima et al. [15] described that glucose metabolism becomes reduced in the posterior cingulate gyrus from the early stage of AD/DLB. Reduced metabolism and blood flow is considered more specific to AD/DLB at this site than at the parietal lobe. The specificity was improved using determination criterion 2, in which a patient is assigned to the AD/DLB group if blood flow is reduced in the ROI for the posterior cingulate gyrus and precuneus, and to the non-AD/DLB group if the reduction is in the parietal lobe ROI.

Visual differentiation by experts

The sensitivity and specificity for visually detecting AD/DLB among patients with mild disease and MMSE scores of ≥24 points was 46.0–90.0 % and 22.2–77.8 %, respectively, indicating greater inter-reader variability than when patients had MMSE scores of 20–23 points. This might be because elder patients with less severe disease have smaller reductions in blood flow and metabolism and do not present typical findings of AD [16], and the raters could not visually determine the significance of the blood flow reduction.

Comparison of visual and ZSAM assessment

One expert rater had significantly higher diagnostic accuracy rates than ZSAM for all patients and those with MMSE scores of 20–23 points (89.2 and 93.1 %, respectively. The diagnostic accuracy rates also did not significantly differ between visual assessment by the other three raters and ZSAM, or the diagnostic accuracy rate by ZSAM was significantly higher. "No significant difference" in a small sample sized study does not mean "really no difference". In order to show real no difference, a power analysis in a larger sample group is required, therefore we may have to increase the number of non-AD/DLB group in our study. In spite of this, evaluations by ZSAM and by expert visual assessment are similarly effective. The results of ZSAM could serve as a diagnostic reference to aid the expert visual interpretation of SPECT images of degenerative dementia.

Limitations

There are some limitations in this study. Because it was impossible to obtain the pathology findings from all the subjects, we had to set the clinical diagnosis as gold standard which has the limitation of diagnostic accuracy: approximately 80 %. Visual inspection of perfusion SPECT for dementia diagnosis does not only depend on the affected regions in the parietal and posterior cingulate cortices but also on the frontal, hippocampal, sensorimotor, cerebellar and other regions. In this study, we focused on only the parietal and posterior cingulate cortices; however, we should analyze other regions for further improvement of our method.

The accuracy of differential diagnosis may be influenced by the constitution of the non-AD/DLB group. In this study most of the diseases were FTD and PSP, but if the numbers of SPA and CBD were large, the results may be different. However, in practical situations the numbers of FTD and PSP are larger than those of SPA and CBD, therefore our findings would not be affected adversely in a clinical situation.

Conclusions

ZSAM using IMP-SPECT and 3D-SSP can differentiate AD/DLB from non-AD/DLB across several institutions, its diagnostic performance is equivalent to that of expert visual assessment, and it might be clinically applicable. We presently use this method as an aid to visual assessment and not as the main diagnostic modality.

Acknowledgments The authors thank Mr. Kiyotaka Watanabe and Mr. Shuya Miki (Nihon Medi-Physics, Tokyo, Japan) for providing and improving the iNEUROSTAT++ program, which uses the 3D-SSP program and was dedicated to this *Z*-score summation analysis method.

Conflict of interest Kazunari Ishii received lecture fees from Nihon Medi-Physics. Kengo Ito, Atsushi Nakanishi, Shin Kitamura, and Akira Terashima declare that they have no conflict of interest.

References

1. Reiman EM, Jagust WJ. Brain imaging in the study of Alzheimer's disease. Neuroimage. 2012;61:505–16.
2. Herholz K. Perfusion SPECT and FDG-PET. Int Psychogeriatr. 2011;23(Suppl 2):S25–31.
3. Ishii K, Kanda T, Uemura T, Miyamoto N, Yoshikawa T, Shimada K, et al. Computer-assisted diagnostic system for neurodegenerative dementia using brain SPECT and 3D-SSP. Eur J Nucl Med Mol Imaging. 2009;36:831–40.
4. Minoshima S, Frey KA, Koeppe RA, Foster NL, Kuhl DE. A diagnostic approach in Alzheimer's disease using three-dimensional stereotactic surface projections of fluorine-18-FDG PET. J Nucl Med. 1995;36:1238–48.
5. McKhann G, Drachman D, Folstein M, Katzman R, Price D, Stadlan E. Clinical diagnosis of Alzheimer's disease: report of the NINCDS-ADRDA Work Group under the auspices of Department of Health and Human Services Task Force on Alzheimer's Disease. Neurology. 1984;34:939–44.
6. McKeith IG, Dickson DW, Lowe J, Emre M, O'Brien JT, Feldman H, et al. Consortium on DLB. Diagnosis and management of dementia with Lewy bodies: third report of the DLB Consortium. Neurology. 2005;65:1863–72.

7. Onishi H, Matsutomo N, Kai Y, Kangai Y, Amijima H, Yamaguchi T. Evaluation of a novel normal database with matched SPECT systems and optimal pre-filter parameters for 3D-SSP. Ann Nucl Med. 2012;26:16–25.
8. Neary D, Snowden JS, Gustafson L, Passant U, Stuss D, Black S. Frontotemporal lobar degeneration: a consensus on clinical diagnostic criteria. Neurology. 1998;51(1):546–54.
9. Litvan I, Agid Y, Calne D, Campbell G, Dubois B, Duvoisin RC, et al. Clinical research criteria for the diagnosis of progressive supranuclear palsy (Steele–Richardson–Olszewski syndrome): report of the NINDSSPSP international workshop. Neurology. 1996;47:1–9.
10. Ishikawa M, Hashimoto M, Kuwana N, Mori E, Miyake H, Wachi A, et al. Guidelines for management of idiopathic normal pressure hydrocephalus. Neurol Med Chir (Tokyo). 2008;48(Suppl):S1–23.
11. Lang AE, Riley DE, Bergeron C. Cortical-basal ganglionic degeneration. In: Calne DB, editor. Neurodegenerative disease. Philadelphia: Saunders; 1994. p. 877–94.
12. Gilman S, Wenning GK, Low PA, Brooks DJ, Mathias CJ, Trojanowski JQ, et al. Second consensus statement on the diagnosis of multiple system atrophy. Neurology. 2008;71:670–6.
13. Calne DB, Snow BJ, Lee C. Criteria for diagnosing Parkinson's disease. Ann Neurol. 1992;32 (Suppl):S125–7.
14. Ishii K, Yamaji S, Kitagaki H, Imamura T, Hirono N, Mori E. Regional cerebral blood flow difference between dementia with Lewy bodies and AD. Neurology. 1999;53:413–6.
15. Minoshima S, Giordani B, Berent S, Frey KA, Foster NL, Kuhl DE. Metabolic reduction in the posterior cingulate cortex in very early Alzheimer's disease. Ann Neurol. 1997;42:85–94.
16. Sakamoto S, Ishii K, Sasaki M, Hosaka K, Mori T, Matsui M, et al. Differences in cerebral metabolic impairment between early and late onset types of Alzheimer's disease. J Neurol Sci. 2002;200:27–32.

平成 24～26 年度　厚生労働科学研究費補助金（長寿科学総合研究事業）
介護予防プログラム開発に関する研究
平成 24～26 度　総合研究報告書

発行責任者　研究代表者　島田　裕之
発　　行　愛知県大府市森岡町 7 丁目 430 番地
国立長寿医療研究センター
TEL　0562－46－8294
FAX　0562－46－8294